Lanthanum-Doped Barium Stannate - a New Type of Critical Raw Materials-Free Transparent Conducting Oxide

D. Gogova[1,*], A. Suwardi[2], Y.A. Kuznetsova[3], A.F. Zatsepin[3], L.A. Mochalov[4], A. Nezhdanov[4] and B. Szyszka[5]

[1]*Central Lab of Solar Energy at the Bulg Acad. Sci., Blvd. Tzarigradkso shose 72, 1784 Sofia, Bulgaria*

[2]*Nanyang Technological University, Singapore*

[3]*Ural Federal University, Mira 19, 620002 Ekaterinburg, Russia*

[4]*Lobachevsky State University of Nizhny Novgorod, Gagarin Ave. 23, 603950 Nizhny Novgorod, Russia*

[5]*Technische Universität Berlin, Fakultät Elektrotechnik und Informatik, Kantstraße 75, 10627 Berlin, Germany*

Abstract: A pulsed laser deposition-based process for growth of highly-doped epitaxial La:BaSnO$_3$(001) layers on (001)-oriented SrTiO$_3$ is developed. The growth window of single-phase epitaxial Ba$_{0.93}$La$_{0.07}$SnO$_3$ films is determined and the influence of growth parameters on crystalline quality is studied.

Reciprocal space maps showed fully relaxed Ba$_{0.93}$La$_{0.07}$SnO$_3$ epitaxial layers on SrTiO$_3$ (001). The crystalline quality of material obtained was evidenced through HR-XRD measurements with a full width at half maximum (FWHM) of 290 arcsec for the Rocking curve of the symmetric (002) peak and 108 arcsec for the asymmetric (103) peak. The band gap of the layers, determined from Reflection measurements employing the Kubelka-Munk method, was estimated as 2.97 - 3.01 eV, *i.e.* very suitable for the applications envisaged. The layers demonstrated electrical conductivity value of 1024 ($\Omega \cdot$cm)$^{-1}$ at a free carrier concentration of 2.18×10^{21} cm^{-3} and a high transparency (up to 90%) in the visible and NIR range of spectrum. The Ba$_{0.93}$La$_{0.07}$SnO$_3$ layers grown could be regarded as a cost-effective and thermally and chemically stable alternative to highly doped ZnO-based transparent conductive oxides and to In$_2$O$_3$:Sn in applications ranging from solar energy utilization to optoelectronics as well as for the emerging field of transparent and radiation hard electronics.

Keywords: Critical raw materials, TCOs, BaSnO$_3$, La doping , Kubelka-Munk method.

1. INTRODUCTION

Wide bandgap semiconductor oxides are among the most challenging materials in the field of science and technology nowadays [1-22]. It is generally believed that high optical transparency is incompatible with high electronic conductivity, since optical transparency requires large optical band-gap while such a large band gap makes carrier doping very difficult. In this sense, transparent conductive oxides (TCOs) are special materials that can simultaneously conduct electricity while having large band-gap. A band-gap energy larger than 3.0 eV and a carrier concentration of the order of 10^{20} cm^{-3} or higher are required for high conductivity and visible light transmittance [9-22]. Such materials are called degenerate semiconductors.

The demand for TCOs films is strongly increasing due to the extensive market growth in these areas, however, the solutions available today only partially fulfill the requirements on low resistivity, high transmittance, large area deposition, low cost manufacturing, and ability for fine patterning, light scattering and precise alignment of the electronic structure to surrounding semiconductors.

Various TCO thin films consisting of highly impurity-doped SnO$_2$ (SnO$_2$:Sb and SnO$_2$:F), In$_2$O$_3$ (In$_2$O$_3$:Sn, or ITO) [11, 12, 14], ZnO (ZnO:Al [9, 11, 12, 18], ZnO:Ga [11, 12]) and TiO$_2$:Nb [21] films have been investigated so far in this field. Among them, ITO is the mostly used in practise since it has the lowest resistivity of the order of 1–2×10^{-4} $\Omega \cdot$cm.

The substitution of the industry standard TCO - ITO - with an earth-abundant, high-performance, cheap, non-toxic, and highly durable against hydrogen plasma compared to ITO alternative material represents a major technological challenge nowadays. The development of a fabrication process for a high-performance TCO material that is meantime cheap will have an important impact on reduced dependency on Critical Raw Materials (CRMs), *i.e* Indium, defined by the European Commission [23] and decreased cost of TCO coatings in a number of large-area applications such as smart windows, photovoltaic devices, liquid crystal displays (LCD), organic and inorganic light-emitting diodes (LEDs), touch panels, etc. [9-22].

Commercial production of TCOs polycrystalline films requires high electrical conductivity with minimal

[*]Address correspondence to this author at the Central Lab of Solar Energy at the Bulg. Acad. Sci., Blvd. Tzarigradkso shose 72, 1784 Sofia, Bulgaria; E-mail: dgogova@abv.bg

degradation in optical transparency during device exploitation. The electrical conductivity of La-doped $BaSnO_3$ at room temperature is about of 1690 S.cm^{-1} [24], which is higher than of industry standard TCOs. The carrier mobility reported in single-crystalline La-doped $BaSnO_3$ is about of 320 cm^2 V^{-1} s^{-1} [24, 25] is the highest value for any TCO and the highest among the perovskite materials. Subsequent work on lanthanum doped barium stannate (LBSO) epitaxial thin films on $SrTiO_3$ (001) (STO) [25] substrates challenged this picture with room temperature mobility (resistivity) of 70 cm^2 V^{-1} s^{-1}, (0.17 mΩ·cm), which are comparable to conventional ITO thin films.

The rapid development of perovskite-based photovoltaic cells requires fast development of compatible transparent electrodes. Titanate-based perovskites have been heavily studied as potential TCOs, however, recently $BaSnO_3$ (BSO) has been proposed as a high mobility TCO because its conduction band is composed of Sn5s orbitals and La doping will create free carriers [24]. The shallow donor states introduced by La-dopant enhance the electrical conductivity leading to blue-shift in the optical transparency, which are ideal for TCO devices. Moreover, the superior durability of stannates thin films compared to ZnO- and SnO_2-based TCOs, regarded as the cheap alternatives to ITO, has already been reported [26].

Pulsed laser deposition technique (PLD) is the method of choice in this study since it is a very versatile and flexible physical vapour phase epitaxial technique allowing achievement of high quality thin film materials [1, 5] with complex and pre-defined compositions due to the stoichiometric transfer from target to the substrate. PLD is as well as a carbon-free method, which avoids complex chemical reactions and inevitable carbon incorporation from organic precursors typical of MOVPE [3] even when the carbon itself does not affect the properties studied [27].

The correlation between the structural, electrical and transmission in the VIS-NIR range of La-doped $BaSnO_3$ (LBSO) epitaxial films was studied to select the optimal conditions for deposition of TCO with the highest figure of merit.

2. EXPERIMENTAL

2.1. Target Preparation

A bulk target with stoichiometric composition of $Ba_{0.93}La_{0.07}SnO_3$ (LBSO) was fabricated by solid state reaction using a mixture of high purity powders of $BaCO_3$, La_2O_3, and SnO_2 (Alfa Aesar) as starting materials. Stoichiometric mixtures were ground, cold pressed and sintered at 1400°C for 24 hours in alumina crucibles.

2.2. Substrate Selection and Preparation

Commercial $SrTiO_3$ (001) with lateral sizes of 5 × 5 mm and a thickness of 0.5 mm is employed as the substrate for the highly doped epitaxial La:BaSnO$_3$ growth since it has the same perovskite structure and similar chemistry. The $SrTiO_3$ substrates were cleaned in ethanol and acetone and dried before deposition.

2.3. Epitaxial Growth

PLD was selected as the method of choice in this study due to its capability to attain high quality crystalline materials at reasonable costs. The growth experiments have been performed in a low-pressure PLD equipment at the Cambridge University, UK. The 248 nm line of a KrF laser with a laser fluency of 2 J/cm^2 and 4 Hz frequency were used. A special mask to ensure energy uniformity in the laser beam was employed. The growth temperature was varied from 650° to 850°C with a step of 50°C and the oxygen pressure from 1 to 40 Pa. A target to substrate distance of 5 cm was maintained. The numbers of pulses were adjusted to grow approximately 100 nm thick films to have a reliable basis for comparison in different experiments. No buffer layer was employed. After growth process the samples were cooled down to room temperature in oxygen atmosphere to prevent any surface decomposition. Some additional ex-situ annealing procedures for 30 and 60 min at a temperature of 900°C in O_2-containing atmosphere were performed to improve the crystallinity and to avoid some oxygen deficiency (formation of oxygen vacancies) in the material typical of PLD growth. After optimization of the growth process parameters (temperature, base pressure, oxygen partial pressure, etc.) and clarification of their impact on the material crystalline quality the optimal set of deposition parameters was selected.

2.4. Characterization

The morphology of the thin film surface was studied by means of atomic force microscopy and the layer chemical composition by EDX in a SEM microscope.

The epitaxial relationship and phase composition of the $Ba_{0.93}La_{0.07}SnO_3$ layers, grown on $SrTiO_3$, was

investigated by X-ray powder diffraction (XRD), while High-resolution XRD experiments (HR-XRD) were carried out to evaluate the material crystalline quality and to record X-ray reciprocal space maps for the epitaxially grown layers and the STO substrates. A Panalytical High Resolution X-ray Diffractometer (with $Cu_{K\alpha}$ radiation, a 2-bounce hybrid monochromator and 0.5 mm slit beam tunnel) was used to determine the crystalline quality of the deposited epitaxial layers.

The phase composition of the PLD target was studied by Raman spectroscopy. The Raman spectroscopy measurements were performed at room temperature in a backscattering geometry using a Horiba Jobin Yvon spectrometer. For excitation, the 488 nm laser line of an Ar laser was employed. The carrier density and mobility in the degenerate semiconductor layers were determined by Hall effect measurements in a van der Pauw configuration of the electrodes.

3. RESULTS AND DISCUSSION

3.1. PLD Target Assessment

Figure **1** illustrates a Raman spectrum of the PLD target sintered by ceramics solid state reactions of propper mixtures of $BaCO_3$, La_2O_3, and SnO_2 powders. The Raman spectrum corresponds to a polycrystalline structure. The peak at 723.87 cm^{-1} is the most intense peak that belongs to the $BaSnO_3$. The Raman peak with a very small intensity at 1060 cm^{-1} is due to residual $BaCO_3$ phase [28]. Storage of $BaSnO_3$ at ambient atmosphere could be the reason for that peak appearance since $BaCO_3$ decomposes at temperatures
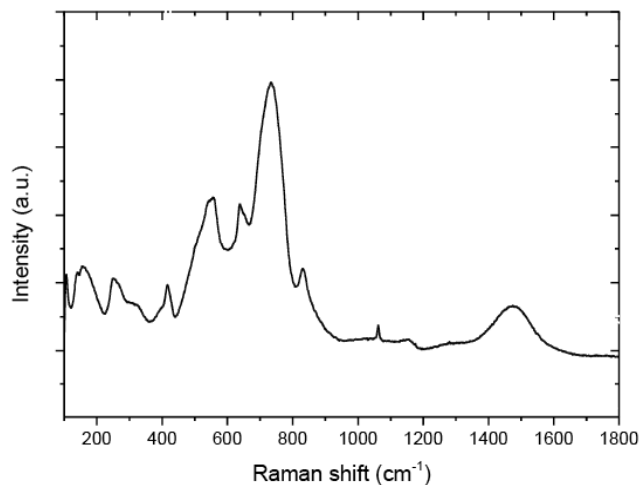
above 1200°C [28] and our sintering temperature was 1400°C.

The expected chemical composition $Ba_{0.93}La_{0.07}SnO_3$ of the PLD epilayers was confirmed by EDX measurements.

3.2. Structural Properties Study

On the basis of thorough process parameters optimization the growth window for deposition of pure phase single-crystalline LBSO layers was determined. All thin films of $Ba_{0.93}La_{0.07}SnO_3$ grown at temperatures ranged from 650°C to 850°C, oxygen partial pressure varied from 1 to 40 Pa and at a laser fluence of 2 J/cm^2 were homogeneous, highly transparent (about 90%) in the VIS and NIR range of spectrum and exhibit a smooth surface morphology (not shown here).

Figure **2** shows 2θ−ω scans of an LBSO epitaxial film on STO substrate as-grown (black) at oxygen partial pressure of 1 Pa with deposition temperature of 850°C as well as a post-annealed sample at 900°C for an hour in oxygen atmosphere (red line). The XRD peak assignment shows the epitaxial relationship between the STO(001) substrate and the PLD grown LBSO(001) layer. The four sharp peaks at 2θ = 21.53°, 43.87°, 68.16° and 96.92° can be identified as the (001), (002), (003) and (004) peaks from the LBSO, respectively [29]. Additionally, substrate peaks from STO (001), (002), (003) and (004) are as labelled. No additional peak are observed, demonstrating the phase purity of the La-doped film. The annealing at 900°C for an hour in oxygen does not introduce changes in the $Ba_{0.93}La_{0.07}SnO_3$ XRD peaks positions, as shown by the RSM.

Figure 1: Raman spectrum of the PLD target prepared by ceramic solid state reactions through sintering of $BaCO_3$, La_2O_3 and SnO_2 powders at a high temperature.
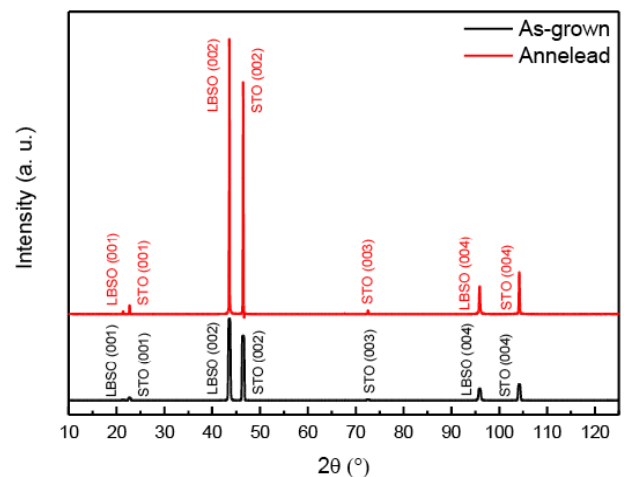

Figure 2: Typical 2θ−ω scans of a LBSO epitaxial layer on STO for as-grown (black) and annealed at 900°C for an hour (red line).

The growth parameter with the strongest impact on the film crystalline quality is the deposition temperature. This was proven by systematic HR-XRD Rocking curve ω-scan measurements. The highest crystalline quality, *i.e.* the lowest FWHM values for the Rocking curves: 290 arcsec of the symmetric (002) peak and 108 arcsec for the asymmetric (103) peak was achieved for the $Ba_{0.93}La_{0.07}SnO_3$ film grown at an oxygen partial pressures of 2 Pa and at the highest deposition temperature – 850°C.

To examine the strain state in the LBSO films, which is especially important in terms of practical applications in multilayer device structures, Reciprocal Space Maps (RSMs) measurements were performed on the (103) reflection of both $SrTiO_3$ substrate and of the LBSO film. Figure **3** shows the RSMs of a sample deposited at oxygen partial pressure of 2 Pa and at the deposition temperature of 850°C as-grown (a) and annealed at 900°C for an hour in oxygen (b). The in-plane as well as out-of-plane lattice parameter can be extracted from the RSMs. The lattice parameters of the $Ba_{0.93}La_{0.07}SnO_3$ film determined from the RSMs are normalized with respect to those of $SrTiO_3$ substrate (3.905 Å) since this is a relative scan. For the as-grown $Ba_{0.93}La_{0.07}SnO_3$ film the in-plane lattice parameter was determined to be 4.132 Å and the out-of-plane lattice parameter to be 4.154 Å.

From the RSM of the same sample after annealing in oxygen-containing atmosphere (Figure **3b**) we have calculated an in-plane lattice parameter of 4.133 Å and an out-of-plane lattice parameter of 4.150 Å. No appreciable difference in the lattice parameter before and after annealing is seen. The only difference is the appearance of a small peak right above film peak in Figure **3b**, which should be La-phase that forms in result of a long-term annealing: at 900°C for an hour. Since the bulk lattice constant of $BaSnO_3$ is 4.115(1) Å, our $Ba_{0.93}La_{0.07}SnO_3$ film are obviously relaxed on STO(001) substrate most likely by formation of misfit dislocations observed by TEM (not shown here).

3.3. Optical Properties Study of the LBSO-Based TCO

Reflection spectra of $BaSnO_3$:La films grown on $SrTiO_3$ substrate have been measured by Lambda 35 spectrophotometer equipped with an integrating sphere. In order to convert the reflection data to the spectral dependences of absorption we used the Kubelka-Munk model [30]:

$$F(hv) = (1 - R(hv))^2 / 2R(hv) \qquad (1)$$

where $F(hv)$ is the Kubelka-Munk function that is directly proportional to the absorption coefficient. To determine the types of transitions responsible for interband absorption we have performed the analysis of absorption data in accordance with Tauc relation [31], using the $F(hv)$ function as analogue of absorption coefficient $\alpha(hv)$:

$$F(hv) \cdot hv = A(hv - E_g)^n \qquad (2)$$

where A is a constant, E_g is the energy gap, *n* is an index depending on the nature of electronic transitions
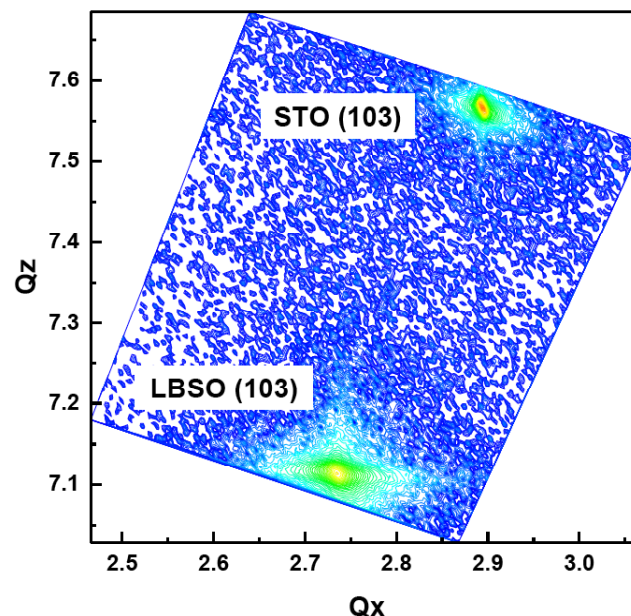

Figure 3a: RSM of a sample deposited at oxygen partial pressure of 2 Pa and at the deposition temperature of 850°C.
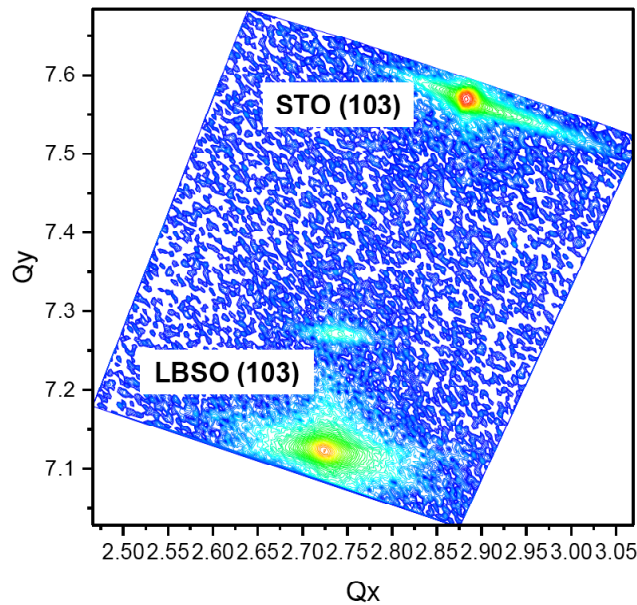
Figure 3b: RSM of the same layer ex situ annealed in oxygen-containing atmosphere for 1 h at 900°C.

that is equal to 1/2, 3/2, 2, 3 for allowed or forbidden direct and allowed or forbidden indirect transitions respectively. It has been established that experimental data for all samples are the best described by Tauc equation when the parameter *n* is fixed as 1/2. This fact indicates the realization of direct allowed transitions in BaSnO₃:La layers regardless of the deposition conditions.

To determine the energy gap values we have plotted the $(F(hv) \cdot hv)^2$ versus photon energy hv as shown in Figure **4**. In obtained dependences the linear regions can be distinguished. Extrapolations of straight lines to the abscissa axis within the allocated regions result in the E_g values that are listed in Table **1**.
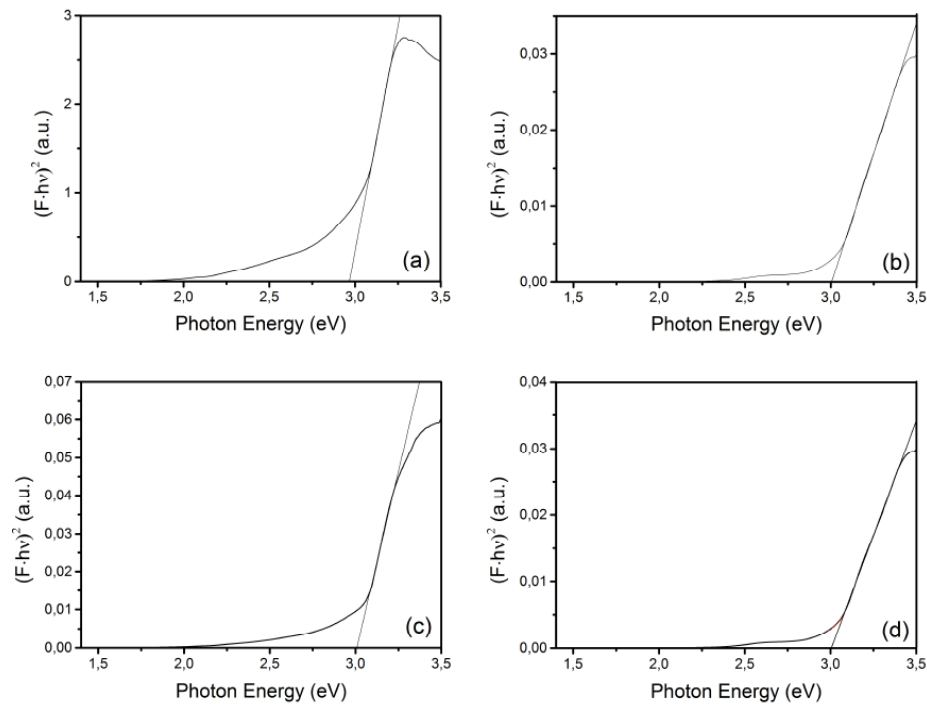

Figure 4 a-d: Absorption spectra in coordinates of Kubelka-Munk function for direct allowed transitions of BaSnO₃:La films grown on SrTiO₃ substrate under different deposition conditions: (**a**) T=650°C, P=10 Pa, (**b**) T=850°C, P=10 Pa, (**c**) T=750°C, P=10 Pa, (**d**) T=750°C, P=5 Pa.

Table 1: Energy Gap Values for BaSnO₃: La Films Grown on SrTiO₃ Substrate Under Different Deposition Conditions

Sample	Substrate Temperature (°C)	Oxygen Pressure (Pa)	Energy Gap (eV)
1	750	5	3.00 ± 0.006
2	750	10	3.01 ± 0.001
3	650	10	2.97 ± 0.003
4	850	10	3.01 ± 0.001

Absorption spectra in coordinates of Kubelka-Munk function for direct allowed transitions demonstrate a number of features. It should be noted that the greatest length of linear regions (3.07 - 3.4 eV) is observed for the samples 2 and 4 that leads to a smaller values of errors in determining of energy gap. In the spectra indicated as (a) and (c), corresponding to samples 1 and 3, the regions of direct interband transitions appear to be smaller (3.1 - 3. 2 eV) that is the reason of higher error of energy gap values. Moreover, in the case of these samples the absorption tails are more extended to the lower photon energies. It can be caused by some extended structural deffects that in turn depends on synthesis conditions. The weak absorption band at 2.6 eV that appeared in all spectra could be associated with optically active defects in the layers investigated. The small difference of the optical band gap values of the different thin film samples is most likely due to some deviation from the nominal stoichiometry (the pre-defined target composition) and/or smaller crystalline perfection of the films grown at lower temperature.

The electrical properties of the $Ba_{0.93}La_{0.07}SnO_3$ layers were characterized by Hall effect measurements. The best of them in terms of crystalline quality demonstrated electrical conductivity value of 1024 $(\Omega \cdot cm)^{-1}$ at a free carrier concentration of 2.18×10^{21} cm^{-3}.

The figure of merit of our LBSO-based TCO was calculated using Ref. 32 as 5×10^{-3} Ω^{-1}. There is still room for improvement. The figure of merit of reactively evaporated ITO thin films increases from 1.14×10^{-3} to 6.4×10^{-3} Ω^{-1} with the increase of the oxygen partial pressure [33].

3.4. Life-Time and Chemical Stabilty Tests

A chemical test of the LBSO-based TCO has carried out in 0.01M HCl/Adipic acid/NaOH solution for 5 min at room temperature. No any change in layer resistance and transmission was observed, confirming the very high stability of BSO against chemicals relevant to production and exploatation.

Life-time durability tests: 3 months exposure to UV light and 1000 h at damp heat (85°C at 85% relative humidity) of the $Ba_{0.93}La_{0.07}SnO_3$ TCO developed have been performed. No any degradation in terms of decrease of trasparency and appearance of optically visible defects has been observed demonstrating the high application potential of this kind of earth-abundant elements-based TCO in PVs, LEDs and smart windows. First plasma treatment experiments of BSO were successfully performed showing very good stability against hydrogen-plasma that is highly desirebale in terms of industrial applications of TCOs.

CONCLUSIONS

A PLD-based process for growth of epitaxial highly-doped by lanthanum BaSnO₃(001) films on (001)-oriented SrTiO₃ is developed. The HR-XRD Rocking curve values achieved demonstrated good crystalline quality.

Experimental results have shown that heavily n-type doped BaSnO₃ is highly promising as a CRM-free and good performance TCO (good conductivity, stability and high optical transparency in the visible and NIR range of spectrum) for applications such as photovoltaic devices, liquid crystal displays, organic and inorganic light-emitting diodes, touch panels, etc. The LBSO can be also easily integrated in device structures (all transparent perovskite devices) with a number of cubic perovskite materials based on the similar chemistry and in-plane lattice parameter.

ACKNOWLEDGEMENTS

REFERENCES

[1]   Macmanus-Driscoll JL, Foltyn SR, Jia QX, Wang H, Serquis A, Civale L *et al*. "Strongly enhanced current densities in superconducting coated conductors of YBa$_2$Cu$_3$O$_{7-x}$+ BaZrO$_3$ " Nature Mater 2004; 3: 439.
https://doi.org/10.1038/nmat1156

[2]   Petrov PP, Miller W and Guhl H. "First atomistic studies of epitaxial growth of Na0.5Bi0.5TiO3 on SrTiO3", Phys. Status Solidi (b) 2008; 245(12): 2649-2656.
https://doi.org/10.1002/pssb.200844246

[3]   Gogova D, Schmidbauer M and Kwasniewski A. "Hetero- and homoepitaxial growth of Sn doped β-Ga2O3 layers by MOVPE", Cryst Eng Comm 2015; 17: 6744-6752.
https://doi.org/10.1039/C5CE01106J

[4]   Zatsepin A, Kuznetsova Y, Spallino L, Pustovarov V and Rychkov V. "Photosensitive defects in Gd2O3 – advanced material for solar energy conversion", Energy Procedia 2016; 102: 144-151.
https://doi.org/10.1016/j.egypro.2016.11.329

[5]   Chen AP, Bi ZX, Tsai CF, Lee J, Su Q, Zhang XH, Quanxi J *et al*. "Tunable Low-Field Magnetoresistance in (La0.7Sr0.3MnO3)0.5:(ZnO)0.5 Self-Assembled Vertically Aligned Nanocomposite Thin Films", Adv Funct Mater 2011; 21: 2423.
https://doi.org/10.1002/adfm.201002746

[6]   Petrov PP and Miller W. "A new Kinetic Monte Carlo Method for the thin film growth of perowskites" Surface Review Lett 2009; 16(06): 909-916.
https://doi.org/10.1142/S0218625X09013475

[7]   Kuznetsova Yu A, Zatsepin AF, Tselybeev RA, Rychkov VN and Pustovarov VA. "Luminescence of rare-earth ions and intrinsic defects in Gd2O3 matrix", J Phys Conf Series 2016; 741(1): 012089
https://doi.org/10.1088/1742-6596/741/1/012089

[8]   Petrov PP, Miller W, Rehse U and Fornari R. "A new method for calculation of island-size distribution in submonolayer epitaxial growth", Appl Mathem Modelling 2011; 35(3): 1331-1336.
https://doi.org/10.1016/j.apm.2010.09.010

[9]   Pimentel A, Fortunato ET, Goncalves A, Marques A, Guas HA, Pereira L *et al*., "Polycrystalline intrinsic zinc oxide to be used in transparent electronic devices" Elsevier, Int. Conf. Polycrystalline Semiconductors - Materials, Technologies, Device Applications 2005; 487(1-2): 21-215.

[10] Szyszka B, Loebmann P, Georg A, Mayd C and Elsaesser C. "Development of new transparent conductors and device applications utilizing a multidisciplinary approach", Thin Solid Films 2010; 518(11): 3109-3114.
https://doi.org/10.1016/j.tsf.2009.10.125

[11] Ellmer K, "Past achievements and future challenges in the development of optically transparent electrodes", Nature Photonics 2012; 6: 809-817.
https://doi.org/10.1038/nphoton.2012.282

[12] Granqvist CG, "Transparent conductors as solar energy materials: A panoramic review", Sol Energy Mater Sol Cells 2007; 91: 1529-1598.
https://doi.org/10.1016/j.solmat.2007.04.031

[13] Gogova DS and Gesheva KA. "Technology Development and Properties of APCVD WO3 Electrochromic Thin Films", in "Thin Film Optical Coatings for Effective Solar Energy

Utilization: APCVD Spectrally Selective Surfaces and Energy Control Coatings", Nova Science Pub. Inc., New York, 2007; 165-210.

[14] Handbook of Transparent Conductors, Eds. Ginley DS, Hosono H, and Paine DC, Springer, New York, 2011.

[15] Gogova D, Harisanova A, Ivanova T, Dimitrova Z and Gesheva K. "Electrochromic behavior of CVD thin tungsten oxide films", J Cryst Growth 1999; 198-199, part 2: 1230-1234.
https://doi.org/10.1016/S0022-0248(98)01051-3

[16] Minami T, "Transparent conducting oxide semiconductors for transparent electrodes", Semicon Sci Technol 2005; 20: 35-44.
https://doi.org/10.1088/0268-1242/20/4/004

[17] Gogova D, Thomas LK and Camin B. "Comparative study of gasochromic and electrochromic effect in thermally evaporated tungsten oxide thin films", Thin Solid Films 2009; 517(11): 3326-3331.
https://doi.org/10.1016/j.tsf.2008.12.020

[18] Dhakal T, Nandur AS, Christian R, Vasekar P, Desu S, Westgate C *et al*. "Transmittance from visible to mid infra-red in AZO films grown by atomic layer deposition system", Solar Energy 2012; 86: 1306-1312.
https://doi.org/10.1016/j.solener.2012.01.022

[19] Gogova D, Gospodinova N, Mokreva P, Gesheva K and Terlemezyan L. "Electrochromic properties of tungsten oxide films grown by chemical vapour deposition", Bulg Chem Commun 2001; 33(2): 189-196.

[20] Dewald W, Sittinger V, Szyszka B, Säuberlich F, Stannowski B, Köhl D *et al*. "Advanced properties of Al-doped ZnO films with a seed layer approach for industrial thin film photovoltaic application", Thin Solid Films 2013; 534: 474-481.
https://doi.org/10.1016/j.tsf.2013.02.027

[21] Seeger S, Ellmer K, Weise M, Gogova D, Abou-Ras D and Mientus R, "Reactive magnetron sputtering of Nb-doped TiO2 films: relation between structure, composition and electrical properties", Thin Solid Films 2016; 605: 44-52.
https://doi.org/10.1016/j.tsf.2015.11.058

[22] Gogova D and Gesheva K. "Preparation and characterization of WO3-based electrochromic cell system", EUROCVD 11 Paris, France, 1997, Eds.: Allendorf MD and Bernard C (The Electrochem Soc, Pennington, NJ), 1997; 97-25: 1482-1489.

[23] "Critical raw materials for the EU", European Commission, June 2010.

[24] Kim HJ, Kim U, Kim TH, Kim J, Kim HM, Jeon BG *et al*. "Physical properties of transparent perovskite oxides (Ba,La)SnO3 with high electrical mobility and at room temperature", Phys Rev B 2012; 86: 165205.
https://doi.org/10.1103/PhysRevB.86.165205

[25] Kim HJ, Kim U, Kim HM, Kim TH, Mun HS, Jeon BG *et al*. "High mobility in a stable transparent perovskite oxide", Appl Phys Express 2012; 5: 061102.
https://doi.org/10.1143/APEX.5.061102

[26] Kim JI, Lee W, Hwang T, Kim J, Lee SY, Kang S *et al*. "Quantitative analyses of damp-heat-induced degradation in transparent conducting oxides", Solar Energy Mater. Solar Cells 2014; 122: 28-286.
https://doi.org/10.1016/j.solmat.2013.12.014

[27] Gogova D, Gesheva K, Kakanakova-Georgieva A and Surtchev M. "Investigation of the structure of tungsten oxide films obtained by chemical vapor deposition", Europ Phys J Appl Phys 2000; 11(3): 167-174.
https://doi.org/10.1051/epjap:2000159

[28] Cerda J, Arbiol J, Dezanneau G, Diaz R and Morante JR. "Perovskite-type BaSnO3 powders for high temperature gas sensor applications", Sensor Actuat B 2002; 84: 21-25.
https://doi.org/10.1016/S0925-4005(02)00005-9

[29] Joint Committee on Powder Diffraction Standards.

[30] Kubelka P and Munk F. "An Article on Optics of Paint Layers", J Tech Phys 1931; 12: 593.

[31] Tauc J, "Amorphous and Liquid Semiconductors" Plenum, New York, 1974: 159.
https://doi.org/10.1007/978-1-4615-8705-7_4

[32] Haacke G, "New figure of merit for transparent conductors", J Appl Phys 1976; 47: 4086.
https://doi.org/10.1063/1.323240

[33] Kaleemulla S, Reddy AS, Uthanna S and Reddy PS. "Physical properties of In2O3 thin films prepared at various oxygen partial pressures", J Alloys Compounds 2009; 479(1-2): 589-593.
https://doi.org/10.1016/j.jallcom.2009.01.003